A Novel Fuzzy Logic Controller For Power Optimisation of Electric Vehicle Induction Motor

Miss. Renuka Rameshvar Pardhi[1], Prof. Kalpesh M. Mahajan[2]
[2] Assistant Professor, Dept of Electrcal
[1, 2] K.C.E. Society's College of Engineering and Management, Jalgaon1(MH) India

Abstract- *Energy efficiency is crucial in electric cars (EVs) and hybrid EVs since the energy storage is constrained. The induction motor efficiency increases with loss minimization, which is in addition to its excellent stability and inexpensive cost. Additionally, while it is functioning at less than full load, it may use more energy than is actually required to carry out its functions. This paper suggests a fuzzy logic control (FLC)-based control approach for use in electric vehicle applications. The initial current amplitude can be increased with FLC controller, and more electricity is saved.Simulation was used to confirm the effectiveness of this control using the MATLAB/SIMULINK software suite. The simulation techniques exhibit good, high-performance outcomes in time-domain response and swift rejection of system-affected disturbance when compared to the standard proportional integral derivative controller. As a result, the induction motor's core losses are drastically decreased, which raises the driving system's efficiency.*

Keywords- Power optimisation, Fuzzy logic,Electric vehicle

I. INTRODUCTION

The EV's environmental, technological, and economic potential have sparked the integration of electrical power and transportation networks in ways that were previously unthinkable [1]. The charge of the batteries—the source of power for the EV traction, control, lighting, and air-conditioning system—is the fundamental link between the two sectors. However, charging the EV via the electrical grid places an additional stress on the utility, especially during peak demand periods [2,3]. Promoting charging from renewable sources is one feasible method for reducing the grid's negative effect. The usage of this type of clean energy is expected to have a positive influence on the environment while also improving the overall charging system efficiency [4,5].

The effectiveness and cost of the drive are significantly impacted by the choice of the electric machine. But any drive, including those that can be incorporated into EVs and hybrid EVs, must have electric machines [7]. The two major machine types that can be used in EVs are synchronous motors and induction motors (IMs) [8]. The following propulsion should be included in the EV-drive motor [6, 9–11]:

- High efficiency to increase driving distance.
- High torque density to provide sufficient driving force during startup, climbing, and accelerating.
- Good flow regulating ability to broaden the static power speed range.

Because of its strength, low cost, and minimal maintenance requirements, the IM is more frequently used for traction drives and is the best choice for EVs [12–15]. However, because of its increased losses in the EV application [16, 17], the machine efficiency suffers. Low energy density, larger weight, longer charging periods, and longer battery life are the most constraining factors to integrating such cars into the transportation system [18]. As a result, EV functioning depends on the best possible usage of energy [19–21]. It is commonly accepted that proportional integral derivative (PID) control, which is used in many industrial drives, is one of the most prevalent units due to its effectiveness and ease of implementation.PID controllers are also employed in industrial applications and are a component of the majority of current control loops [22, 23]. Due to component obsolescence or a change in the working environment, significant performance loss may happen when the operation conditions are changed [24]. Fuzzy logic control (FLC), for example, is an intelligent control technique that can be used to deliver superior performance due to the uncertainty and complexity of modelling the accurate analytical model of a controlled system [25–27].

Many strategy rules in the FLC framework make simpler use of linguistic tags. Numerous additional EV energy demand management projects have followed this strategy [6]. A mathematical model of a controlled system is not necessary for FLC because it is a model-free technique [27, 28]. Therefore, the FLC system controller should be created with adaptive features when the system reaches areas with fixed mistakes in order to improve the performance of the EV traction. Other FLC trends include finding appropriate trade-

offs between quick ascending time, minimum steady-state error, and minimum overshoot [29].

The focus of the current design methodologies, however, is on minimising steady-state losses [30, 31]. When typical induction machines are built for high stability efficiency, high and excessive current peak losses in the machine can happen during transit with variable flow linkages. Therefore, the focus of this research is on the losses of transient machines that happen during the extremely dynamic driving cycle that an EV's traction motor drive often experiences.

Numerous various control structures have been offered for EV applications in the literature. These include basic linear methods such sliding mode control [35], direct torque control [33, 34], and field oriented control [7, 32]. Use the model reference adaptive system with an optimised base power scheme, also known as the golden section approach [32], to reduce secondary winding harmonic losses. Using slip control, which is carried out through a fuzzy controller with nine rules, taking speed error change as input, to produce frequency, as well as search controller (SC), which is based on adaptive quadratic interpolation to optimise the loss of IM drive [19].

For EV applications, an FLC-based technique is put forth in this paper. The influence of each of the controllers (PID and FLC) on the performance of IM is then compared. The following is a summary of the important contributions made by this work: At projected speeds and above, the main concern is to reduce the cost of the drive life cycle, and efficiency is a sign of the cost of energy. The overall drive efficiency has an impact on the inverter's efficiency.

II. PROPOSED SYSTEM

As seen in Fig. 1, a battery EV is an electrically powered vehicle that has three basic components: an electric motor system, which is typically just one electrical machine and is typically a three phase AC. via the gearbox and differential, which are coupled to the wheel. The second component is a battery that serves as a power source and is connected to the gadget via an electrical DC/AC power adapter along with the control system. The energy is chemically stored in the battery. Last but not least, the electric machine is equipped with a three-phase frequency and voltage control system that is connected to the accelerator and/or brake pedals based on the wishes of the current driver.

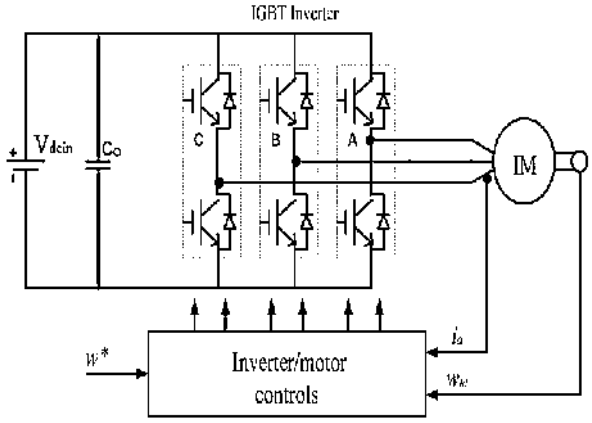

Fig. 1: Induction motor drive for EV

Table 1: Parameters of IM

Parameter	**Value**
Power	37.3 kW
Voltage	460 V
Poles	4
Frequency	50 Hz
Rated Speed	1500 rpm

The three-phase electric machine in Fig. 1 gives the wheels traction power. Torque for the left and right wheels will be provided by the differential with the gear ratio for high-speed adjustment of the electric motor shaft to the low speed of the wheels. An inverter, which changes the battery voltage from DC to three-phase AC voltage, regulates the machine's speed. When analysing the power consumption of an EV that is not a part of the power chain from the grid to the wheels, it is crucial to take component losses into account. Our dedication is to develop adequate controllers for feedback in order to push the EV system into the required operation.By using FLC approaches for EV applications, the controller that is insufficiently flexible, adaptive, and powerful can be created. Table 1 displays the induction motor's parameters that were taken into consideration.

III. CONTROL STRATEGIES

3.1 PID Control:

In the first design approach, a traditional PID controller is introduced for use with an indirect field-oriented IM order to control its speed and also starting scenario is studied. The suggested control system has a phase-locked loop algorithm that synchronises with the utility current regulator and (direct-quadrature-zero) conversion equations. The a-b-c coordinates of the phase currents (ia, ib, and ic) are transformed into a d-q frame. The components of *d–q* can be described using the following conversions:

$$\begin{matrix} id \\ iq \end{matrix} = \sqrt{\frac{2}{3}} X \begin{matrix} \sin(\omega t) & \sin(\omega t - \frac{2\pi}{3}) & \sin(\omega t + \frac{2\pi}{3}) \\ \cos(\omega t) & \cos(\omega t - \frac{2\pi}{3}) & \cos(\omega t + \frac{2\pi}{3}) \end{matrix} X \begin{matrix} ia \\ ib \\ ic \end{matrix}$$

Now, oscillation and average components are taken into account while calculating active and reactive power. To obtain the average components to the outputs of the active power and reactive power, two outside PID control loops are used. Fig. 3 provides a block diagram of the traditional PID control. This PID produces active current reference (*id**) and reactive current reference (*iq**), as given in the following conversions:

$$id^* = k_p(P_{ref} - P) + k_i \int (P_{ref} - P)dt$$
$$iq^* = k_p(Q_{ref} - Q) + k_i \int (Q_{ref} - Q)dt$$

where *k* p is the proportional constant and ki is the basic constant, for the PID controllers used. Pref is the reference for the charging power, and Qref is the reference for the reactive power that the AC source needs. The inner current loop and the outer voltage loop are integrated to provide the control. The current reference, which is used to control the inner loop, is created by comparing the current reference with the actual current in the outer loop. As a result, the Park conversion is used to compare the observed line currents to create the internal PID loops. The results (edand eq) are first summarised by the disengagement conditions and then normalised by the DC voltage to obtain the operating ratios in the d–q coordinates as follows:

$$\begin{matrix} d_d \\ d_q \end{matrix} = \frac{1}{V_{dc}} X \begin{matrix} e_d & v_d & 3\omega L \\ e_q & v_q & -3\omega L \end{matrix} X \begin{matrix} i_q \\ i_d \end{matrix}$$

Inverse matrix transformation can be used to obtain the duty ratios in (*a–b–c*) frame coordinates, which can be expressed as follows:

$$\begin{matrix} D_a \\ D_b \\ D_c \end{matrix} = \sqrt{\frac{2}{3}} X \begin{matrix} \sin(\omega t) & \cos(\omega t) \\ \sin(\omega t - \frac{2\pi}{3}) & \cos(\omega t - \frac{2\pi}{3}) \\ \sin(\omega t + \frac{2\pi}{3}) & \cos(\omega t + \frac{2\pi}{3}) \end{matrix} X \begin{matrix} d_d \\ d_q \end{matrix}$$

3.2 Fuzzy Logic Control:

Controlling this issue continues to be challenging due to the non-linear properties of AC motors, particularly the squirrel cage induction motor (SCIM), as numerous parameters (mostly rotor resistances) fluctuate depending on the operating conditions. For EV applications, traditional control technology (PID) must be modified using the efficient intelligent FLC [37]. The following variables must be taken into account when designing any fuzzy system:

- Generating fuzzy rules for some control concerns, which are developed by subject-matter experts;
- Choosing the membership functions and modifying them; and
- Choosing the scaling factors.

The basic FLC was created for EV applications using the second design strategy. It is a sort of variable structure control unit that has a solid reputation for stability and longevity. Figure 4 depicts an example FLC.

Using the mathematical method known as fuzzy logic, a novel method is offered to enhance the voltage, frequency, and current regulation of adjustable speed drives. It can be used in EV applications to solve issues that render non-linearity and its dynamic nature unmanageable by traditional control approaches. All of the features of this kind of issue are present in motor control.

3.3 Speed Control:

The motor speed error (we) and its derivative, which reflects the speed variation error (we), are required as two input variables for FLC in the case of motor speed control. Speed error and speed variation error could be described as follows:

$$\omega_e = \omega^*_{ref} - \omega_{act}$$
$$\frac{d\omega e}{dt} = \frac{\Delta\omega e}{Ts}$$

The controller output is the incremental change of the control signal Δu. The control signal can be obtained by:

$$\Delta u = \Delta t^*_e = k1.\omega e + k2.\omega e$$

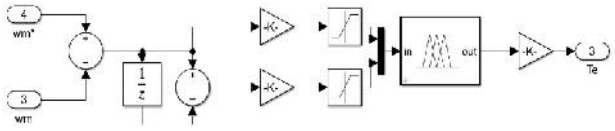

Fig. 2: Fuzzy Logic Controller

where k1 and k2 stand for the system's present and past states, respectively. The world of discourse is defined on the normalised domain [-1, 1] for all membership functions of the controller inputs, we and we, and the output, u, as illustrated in Fig. 5.

The fuzzy logic membership functions have been divided into five groups, as illustrated in Fig. 5, with five membership functions (MF) for inputs and five MF for output fuzzy sets.

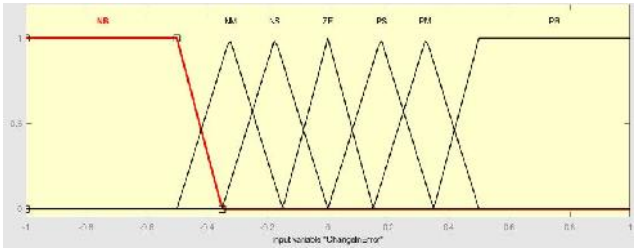

Fig. 3: Membership function for error

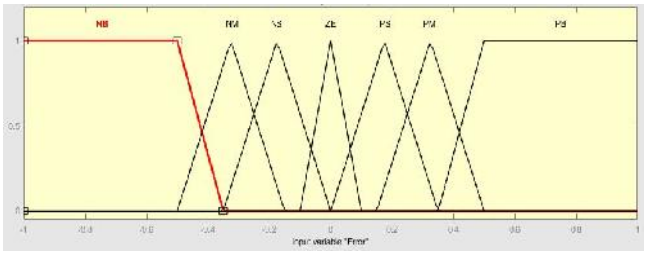

Fig. 4: Membership function for change in error

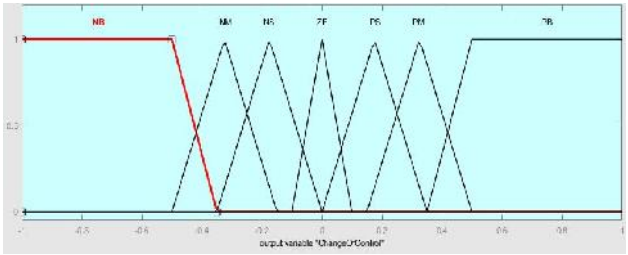

Fig. 5: Membership function for output

In this system, a mamdani fuzzy inference system is utilised to associate two input variables to one output variable. The error (we), which is the difference between the desired (set-point) and measured speed, and the change of error (we), are the two input variables. The normalisation and denormalization of the individual variables of a traditional control gain are carried out via the scaling factors Ge, Gde, and Gu in Fig. 4. The value of these measurement factors is predicated on the starting error when Ge, Gde, and Gu are the error measurement, error variation, and FLC output factors, respectively.While the FLC rules are registered in Table 1, limited models are used to reduce the error and fluctuation in the error between the input and output functions of the FLC, as illustrated in Fig. 5. This characteristic suggests that rather than just interpreting NB, NS, Z, PS, and PB to stand for negative big, negative small, zero, positive small, and positive big, respectively, a more accurate continuous control rule may be created by interpolating the basic table of rules. Here, symmetrical triangles with equal bases and 50% overlap with neighbouring MFs are picked, with the exception of two obscure groups at the outer ends (trapezoidal MFs are chosen).

As shown in Table 2, there are five fuzzy subsets for each variable, which gives 25 possible rules, where the typical rule is: 'If *e* is NB and *de* is PB Then *u* is *Z*'.

Table 2: Rule base for FLC

Δ*we*	*we*				
	NB	NS	Z	PS	PB
NB	NB	NB	NS	NS	Z
NS	NB	NS	NS	Z	PS
Z	NS	NS	Z	PS	PS
PS	NS	Z	PS	PS	PB
PB	Z	PS	PS	PB	PB

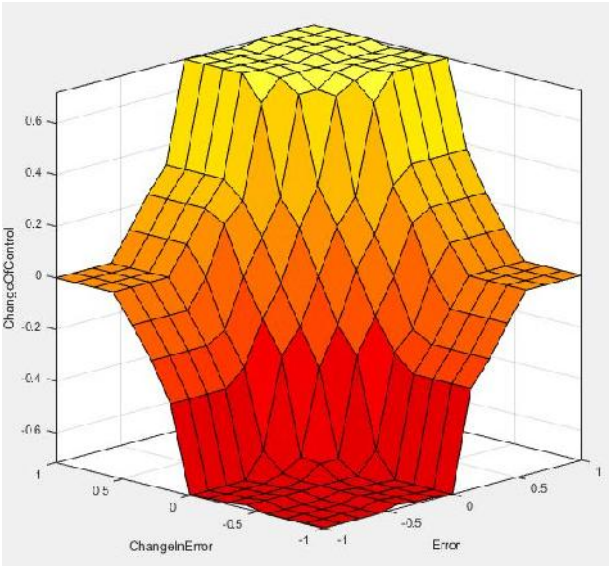

Fig. 6: Surface view of the rule base

Because the perturbation approach changes the motor speed and output power, speed correction control is required. The output rotor speed of the motor should be kept as steady as feasible. Figure 6 depicts the FLC's input/output mapping.

By utilising this fuzzy controller in the outer loop and using the speed error and variation of error as input signals to build the corresponding control terms, it is possible to achieve smooth torque and an improvement in the system performance for EV applications.

IV. INDUCTION MOTOR EFFICIENCY CALCULATION

To confirm the measured efficiency, the following power losses of the suggested control strategy under worst-case conditions are evaluated.

Using PID, three-phase IM draws 22.6 A at 0.85 PF lagging, and FLC, 20 A at 0.85 PF lagging. The expected input power losses are as follows:

$$P_{in} = \sqrt{3} X V_L I_L cos\theta$$

It is taken into account that the stator copper losses are 2 kW and the core losses are 1.8 kW. One estimate for the air-gap power losses is as follows:

$$P_{AG} = Pin - (Pscl + Pcore)$$
$$P_{AG} = Pconv + Prcl = 3I_2^2 \frac{R2}{S} = \frac{Prcl}{S}$$

The only rotor copper losses that are taken into account when converting power are 700 W. The estimated converted power losses are as follows:

$$P_{conv} = P_{AG} - Prcl = (1 - S)P_{AG}$$

The calculation makes the assumption that stray losses are minimal, therefore friction and windage losses are taken into consideration at 600 W each. Table 3 provides an estimation of the output power losses:

$$P_{out} = P_{conv} - (P_{f+w} + P_{stray})$$

Fig. 7 plots the IM drive's efficiency vs the percentage of load. When the IM performs at its best, the energy efficiency rises according to this figure. A more deserving performance is attained by the proposed rules when compared to the results obtained by the controller tuned utilising some well-known tuning rules.

V. SIMULATION AND RESULTS

Two situations are taken into account in the simulation, which is done using the MATLAB software's Simulink toolbox (see Fig. 7). In the first case study, a PID controller is used to power a 50 hp IM. In the first six seconds of operation, three-phase voltage and current are monitored and plotted. We have operated the motor at 1000, 770, and 550 rpm because we are focusing on loss minimization at lighter loads. Figs. 9–11 display the comparison between PID controller response and FLC response.

The vehicle is entirely halted at time t = 0, and the accelerator is abruptly depressed to 70 percent. The car decelerates to 50% at time t = 2 s then to 35% at time t = 4 s.

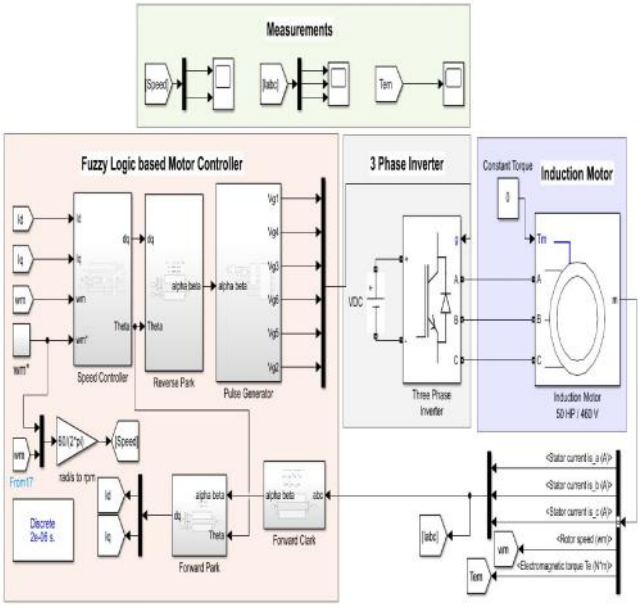

Fig. 7: MATLAB Model

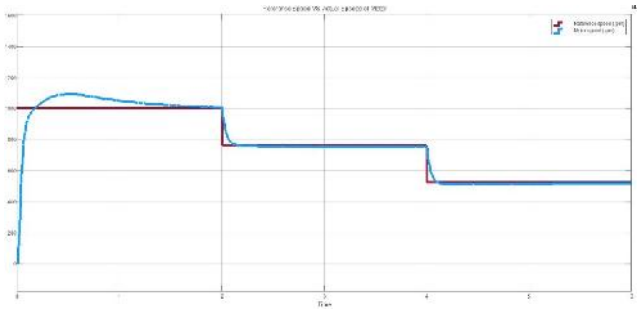

Fig. 8: Speed response with PID controller

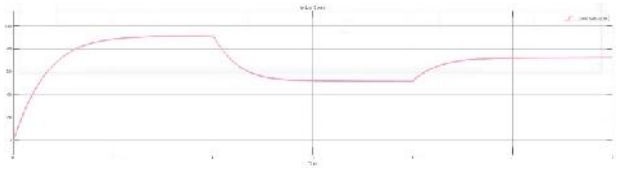

Fig. 9: Speed response with FLC controller

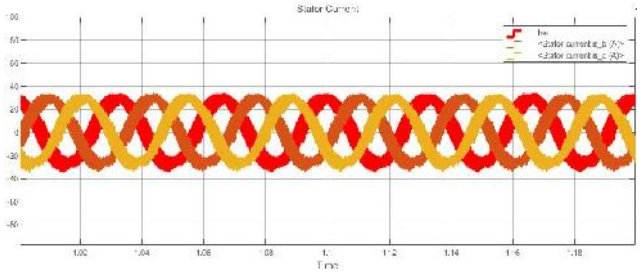

Fig 10: Stator current for FLC controller

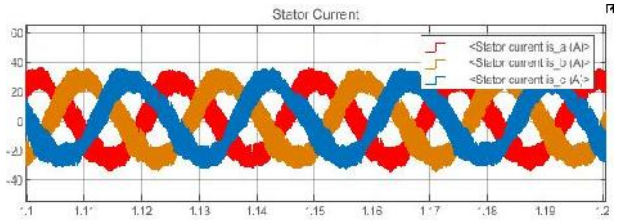

Fig 11: Stator current for PID controller

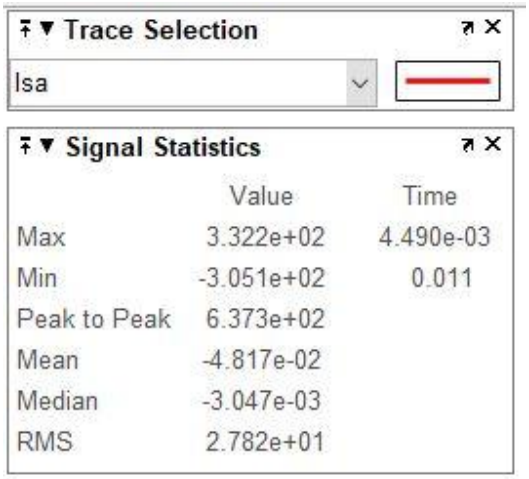

Fig 12: Stator current statistics for FLC

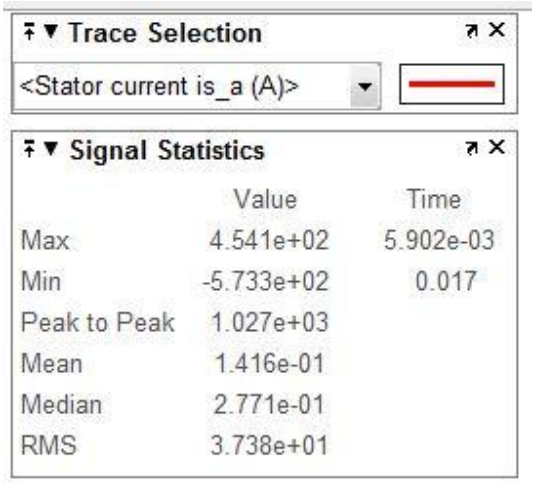

Fig 13: Stator current statistics for PID controller

Fig. 14: Efficiency comparison between two controllers

The outputs and time response of acceleration have improved based on the provided data for the magnitude of starting currents. The suggested method produces a phase current with fewer loss components in the same order of components. PID and FLC were both used in several simulation studies to regulate the IM speed. The control unit's performance results were evaluated by gradually changing the speed reference while maintaining a fixed load torque. The FLC demonstrated a better capacity to manage the three-phase IM's speed and to deliver a precise and quick response with little to no steady state error and no overshoot.

VI. CONCLUSION

IM can use more power than necessary if it is operating at less than full load. Heat is the result of this extra power. More power can be saved during this period by using the FLC to adjust the initial current amplitude. The speed error and change of error are the inputs to the fuzzy controller, which are employed in the outer loop to create an equivalent controller term. In this paper, a simulation analysis using a 50 hp IM-driven EV was carried out.The findings demonstrated that the suggested system's phase current had less loss (reduced amplitude) while maintaining the same order components. For the real torque in the steady state, the loss amplitudes are generally minimised. It accomplishes smooth torque and raises system efficiency. The simulation results of the proposed FLC scheme demonstrated very strong stability and superior performance in terms of rising time, settling time, and peak overshoot compared to the traditional PID controller.

REFERENCES

[1] Galus MD, Andersson G. Demand management of grid connected plug-in hybrid electric vehicles (PHEV). Energy 2030 Conference. ENERGY 2008. IEEE, 2008

[2] Kelman C. Supporting increasing renewable energy penetration in Australia – the potential contribution of

electric vehicles, 2010 20th Australasian Universities Power Engineering Conference (AUPEC). 2010.

[3] Lindgren J, Niemi R, Lund PD. Effectiveness of smart charging of electric vehicles under power limitations. International Journal of Energy Research 2014; 38(3):404–414.

[4] De Schepper E, Van Passel S, Lizin S. Economic benefits of combining clean energy technologies: the case of solar photovoltaics and battery electric vehicles.International Journal of Energy Research 2015; 39(8):1109–1119.

[5] Ben Salah C, Ouali M. Energy management of a hybrid photovoltaic system. International Journal of Energy Research 2012; 36(1):130–138.

[6] Trovao, J.P.F., Roux, M.-A., Menard, E., *et al.*: 'Energy and power-split management of dual energy storage system for a three-wheel electric vehicle', *IEEE Trans. Veh. Technol.*, 2017, **66**, (7), pp. 5540–5550

[7] Buyukdegirmenci, V.T., Bazzi, A.M., Krein, P.T.: 'Evaluation of induction and permanent-magnet synchronous machines using drive-cycle energy and loss minimization in traction applications', *IEEE Trans. Ind. Appl.*, 2014, **50**, (1), pp. 395–403

[8] Sarigiannidis, A.G., Beniakar, M.E., Kladas, A.G.: 'Fast adaptive
evolutionary PM traction motor optimization based on electric vehicle drive cycle', *IEEE Trans. Veh. Technol.*, 2016, **66**, (7), pp. 5762–5774

[9] Wang, Q., Niu, S., Luo, X.: 'A novel hybrid dual-PM machine excited by AC with DC bias for electric vehicle propulsion', *IEEE Trans. Ind. Electron.*, 2017, **64**, (9), pp. 6908–6919

[10] Boukadida, S., Gdaim, S., Mtiba, A.: 'Sensor fault detection and isolation based on artificial neural networks and fuzzy logic applicated on induction motor for electrical vehicle', *Int. J. Power Electron. Drive Syst.*, 2017, **8**, (2), pp. 601–611

[11] Varghese, S.T., Rajagopal, K.R.: 'Economic and efficient induction motor controller for electric vehicle using improved scalar algorithm'. IEEE 1st Int. Conf. on Power Electronics, Intelligent Control and Energy Systems (ICPEICES), Delhi, 2016, pp. 1–7

[12] Ulu, C., Korman, O., Komurgoz, G.: 'Electromagnetic and thermal analysis/ design of an induction motor for electric vehicles'. The 8th Int. Conf. on Mechanical and Aerospace Engineering (ICMAE), Prague, 2017, pp. 6–10

[13] Ouchatti, A., Abbou, A., Akherraz, M., *et al.*: 'Sensorless direct torque control of induction motor using fuzzy logic controller applied to electric vehicle'. Int. Renewable and Sustainable Energy Conf. (IRSEC), Ouarzazate, 2014, pp. 366–372

[14] Makrygiorgou, J.J., Alexandridis, A.T.: 'Induction machine driven electric vehicles based on fuzzy logic controllers'. The 42nd Annual Conf. of the IEEE Industrial Electronics Society, Florence, 2016, pp. 184–189

[15] Li, H., Klontz, K.W.: 'Rotor design to reduce secondary winding harmonic loss for induction motor in hybrid electric vehicle application'. IEEE Energy Conversion Congress and Exposition (ECCE), Milwaukee, WI, 2016, pp. 1–6

[16] Kumar, R., Das, S., Chattopadhyay, A.K.: 'Comparative assessment of two different model reference adaptive system schemes for speed-sensorless control of induction motor drives', *IET Electr. Power Appl.*, 2016, **10**, (2), pp. 141–154

[17] Saleeb, H., Sayed, K., Kassem, A., *et al.*: 'Power management strategy for battery electric vehicles', *IET Electr. Syst. Transp.*, 2019, **9**, (2), pp. 65–74

[18] Das, S., Pal, A., Manohar, M.: 'Adaptive quadratic interpolation for loss minimization of direct torque controlled induction motor driven electric vehicle'. IEEE 15th Int. Conf. on Industrial Informatics (INDIN), Emden, 2017, pp. 641–646

[19] Sayed, K., Abo-Khalil, A.G., Alghamdi, A.S.: 'Optimum resilient operation and control dc microgrid based electric vehicles charging station powered by renewable energy sources', *Energies*, 2019, **12**, (22), p. 4240

[20] Sayed, K., El-Zohri, E., Naguib, F., *et al.*: 'Performance evaluations of interleaved ZCS boost DC-DC converters using quasi-resonant switch blocks for PV interface', *IOSR J. Electr. Electron. Eng., (IOSR-JEEE)*, 2015, **10**, (4), pp. 105–113.

[21] Sayed, K., Gabbar, H.A.: 'Electric vehicle to power grid integration using three-phase three-level AC/DC converter and PI-fuzzy controller', *Energies*, 2016, **9**, p. 532.

[22] Jasim, B.H., Dakhil, A.M.: 'New PI and PID tuning rules using simple analytical procedure'. The Second Scientific Engineering Conf., Mousil, Iraq, 2014

[23] Lin, W.-S., Huang, C.-L., Chuang, M.-K.: 'Hierarchical fuzzy control for autonomous navigation of wheeled robots', *IEE Proc., Control Theory Appl.*, 2005, **152**, (5), pp. 598–606

[24] Chan, C.: 'An overview of electric vehicle technology', *Proc. IEEE*, 1993, **81**, (9), pp. 1202–1213

[25] Wang, S.-C., Liu, Y.-H.: 'A modified PI-like fuzzy logic controller for switched reluctance motor drives', *IEEE Trans. Ind. Electron.*, 2011, **58**, (5),pp. 1812–1825

[26] Kalogirou, S.A.: 'Artificial intelligence for the modeling and control ofcombustion processes: a review', *Prog. Energy Combust. Sci.*, 2003, **29**, (6), pp. 515–566

[27] Mansour, M.F.: 'Design of an adaptive fuzzy controller through sliding mode concept'. PhD thesis, Faculty of Engineering, Mansoura University, 2005

[28] Panicker, D.K., Mol, M.R.: 'Hybrid PI-fuzzy controller for brushless DC motor speed control', *IOSR J. Electr. Electron. Eng. (IOSR-JEEE)*, 2013, **8**,(6), pp. 33–43

[29] Huang, H., Chang, L.: 'Continuous defuzzification of fuzzy logic controller in electric vehicle induction motor drives'. IEEE Int. Conf. on Systems, Man and Cybernetics. Intelligent Systems for the 21st Century, Vancouver, BC, Canada, 1995, vol. 3, pp. 2466–2471

[30] Shi, Y., Lorenz, R.D.: 'Induction machine design for dynamic loss minimization along driving cycles for traction applications'. IEEE Energy Conversion Congress and Exposition (ECCE), Cincinnati, OH, 2017, pp. 278–285

[31] Chrenko, D.: 'Influence of hybridization on eco-driving habits using realistic driving cycles', *IET Intell. Transp. Syst.*, 2015, **9**, (5), pp. 498–504

[32] Pal, A., Das, S.: 'A new sensorless speed estimation strategy for induction motor driven electric vehicle with energy optimization scheme'. IEEE 1st Int. Conf. on Power Electronics, Intelligent Control and Energy Systems (ICPEICES), Delhi, 2016, pp. 1–6